arXiv:1605.02574v1 [astro-ph.SR] 9 May 2016

Bipolar rings from jet-inflated bubbles around evolved binary stars

Muhammad Akashi[1] **& Noam Soker**[1]

ABSTRACT

We show that a fast wind that expands into a bipolar nebula composed of two opposite jet-inflated bubbles can form a pair of bipolar rings around giant stars. Our model assumes three mass loss episodes: a spherical slow and dense shell, two opposite jets, and a spherical fast wind. We use the FLASH hydrodynamical code in three-dimensions to simulate the flow, and obtain the structure of the nebula. We assume that the jets are launched from an accretion disk around a stellar companion to the giant star. The accretion disk is assumed to be formed when the primary giant star and the secondary star suffer a strong interaction accompanied by a rapid mass transfer process from the primary to the secondary star, mainly a main sequence star. Later in the evolution the primary star is assumed to shrink and blow a fast tenuous wind that interacts with the dense gas on the surface of the bipolar structure. We assume that the dense mass loss episode before the jets are launched is spherically symmetric. Our results might be applicable to some planetary nebulae, and further emphasize the large variety of morphological features that can be formed by jets. But we could not reproduce some of the properties of the outer rings of SN 1987A. It seems that some objects, like SN 1987A, require a pre-jets mass loss episode with a mass concentration at mid-latitudes.

Key words: binaries: general - stars: AGB and post-AGB - stars: jets - stars: mass-loss - (ISM:) planetary nebulae: general

1. INTRODUCTION

Bipolar nebulae around evolved stars, such as planetary nebulae (PNe), are thought by many researchers to be shaped by jets that inflate bubbles inside a dense wind, (e.g, Morris 1987; Corradi & Schwarz 1993; Sahai & Trauger 1998; García-Segura et al. 2005; Soker 2007; García-Díaz et al. 2008; Akashi & Soker 2008a; Dennis et al. 2008, 2009; Lee et al. 2009; Velázquez et al. 2011; Boffin et al. 2012; Huarte-Espinosa et al. 2012; Akashi & Soker 2013; Balick et al. 2013; Thomas et al. 2013; Riera et al. 2014; Tocknell et al. 2014; Velázquez et al. 2014; Zijlstra 2015). These bubbles can lead to other morphological features such as a dense equatorial outflow (Soker & Rappaport 2000; Akashi & Soker 2008b; Akashi et al. 2015). The rich variety of outflow types, such as slow winds and fast winds that can be blown, before, during, and after the jets-launching episodes, and the rich variety of interacting binary (Soker 1998; De Marco 2015) and triple (Soker 2016) stellar systems ensure the rich variety of descendant nebular morphologies, practically making almost every bipolar nebula 'unique' (Soker 2002b).

Some of these nebulae contain one pair of bipolar rings (double-rings) e.g., SN 1987A (e.g. Burrows et al. 1995; Panagia et al. 1996; Crotts & Heathcote 2000; Maran et al. 2000; Sugerman et al. 2005) and the PN He 113 (Sahai et al. 2000), while some others contain several rings in each lobe, e.g., the PNe MyCn 18 (Sahai et al. 1999) and NGC 6881 (Kwok & Su 2005), and the Red Rectangle post-AGB nebula (Cohen et

[3]Department of Physics, Technion – Israel Institute of Technology, Haifa 32000 Israel; akashi@physics.technion.ac.il; soker@physics.technion.ac.il.

al. 2004). In SN 1987A the two bipolar rings are referred to as the outer rings. The line connecting the centers of the rings is displaced from the exploding star. Several scenarios for the formation of the outer rings of SN 1987A have been proposed over the years (e.g., Soker 1999, 2002a; Tanaka & Washimi 2002; Sugerman et al. 2005; Morris & Podsiadlowski 2007, 2009). In the present study we aim at producing one pair of bipolar rings from a spherically symmetric fast wind that expands into bipolar jets-inflated bubbles.

Formation of rings by jets interacting with CSM were studied before. Soker (2002a) suggested the formation of double-ring systems from jets interacting with thin dense shells. As a jet interacts with the thin shell a high pressure region is formed, that in turn accelerates the shells material sideways. This process forms a ring. The dense shells are formed from an impulsive mass-loss episode. According to this scenario, due to the binary interaction and its orbital motion the double-ring system is displaced from the symmetry axis of the main nebula, as observed in SN 1987A. Soker (2005) proposed a scenario where repeated jet-launching episodes from a mass-accreting stellar companion form the multiple double-ring system of the Red Rectangle. The jets expand into the dense AGB wind close to the binary system. Martínez González et al. (2015) argue that precessing jets are required to shape the Red Rectangle rather than wide jets. We note that the central star of the Red Rectangle is a post-AGB star (e.g., Van Winckel 2004), and hence no phase of fast wind followed the formation of the rings. In the present study we include a fast wind, hence the presently studied scenario does not apply to the Red Rectangle. Dennis et al. (2008) were aiming at several rings structure, and simulated the formation of rings by launching bullets instead of a continuous jet. Dennis et al. (2009) further found that rings are formed in jet-inflated lobes when magnetic fields are included, but not without magnetic fields.

Although there are recent models for forming bipolar nebulae without jets (e.g., Chen et al. 2016), we attribute the formation of bipolar nebulae to jets. As well, we assume that magnetic fields do not play a significant role in the shaping process far from the source of the winds and jets, and will present pure gas-dynamical simulations. The numerical set up is described in section 2, the results are presented in sections 3 and 4, and our short summary is in section 5.

2. NUMERICAL SET UP

Our simulations are performed by using version 4.0-beta of the FLASH code (Fryxell et al. 2000). The FLASH code is an adaptive-mesh refinement (AMR) modular code used for solving hydrodynamics or magnetohydrodynamics problems. Here we use the unsplit PPM (piecewise-parabolic method) solver of FLASH. We neither include gravity, as velocities are much above the escape speed in the region we simulate, nor radiative cooling, as the interaction region is optically thick. Instead of calculating radiative cooling and radiative transfer, that are too complicated for the flow geometry, we take low values of the adiabatic index, $\gamma = 1.02$ and $\gamma = 1.1$ to mimic radiative cooling via photon diffusion. Using lower values of $\gamma < 5/3$ to mimic radiative cooling is reasonable when kinetic energy is channelled to thermal energy, but not when thermal energy is channelled to kinetic energy. For more details on the numerical settings and the justifications for the parameters employed in this study see Akashi & Soker (2013).

We employ a full 3D AMR (8 levels; 2^{11} cells in each direction) using a Cartesian grid (x, y, z) with outflow boundary conditions at all boundary surfaces. We take the $x - y$ plane with $z = 5 \times 10^{15}$ cm to be in the equatorial plane of the PN, and we simulate the whole space (the two sides of the equatorial plane).

At $t = 0$ we place a spherical dense shell in the region $R_{\rm in} = 10^{14}$ cm $< {\rm r} < 2 \times 10^{14}$ cm $= {\rm R_{out}}$, and with a density profile of $\rho_s = 4.74 \times 10^{-11} (r/10^{14} \text{ cm})^{-2}$ g cm^{-3}, such that the total mass in the shell is

$0.3M_\odot$. The gas in the shell has an initial radial velocity of $v_s = 10$ km s^{-1}. The shell corresponds to a mass loss episode lasting for about 3 yr and with a constant mass loss rate of $\dot{M}_s \simeq 0.1M_\odot$ yr^{-1}. Such an event can be classified as an intermediate luminosity optical transient (ILOT; Soker & Kashi 2012; Akashi & Soker 2013, where more details can be found). The regions outside and inside the dense shell are filled with a lower density spherically-symmetric slow wind having a uniform radial velocity of $v_{\rm wind} = v_s = 10$ km s^{-1}. The slow wind density at $t = 0$ is taken to be $\rho(t = 0) = \dot{M}_{\rm wind}(4\pi r^2 v)^{-1}$, where $\dot{M}_{\rm wind} = 10^{-5}{\rm M}_\odot$ yr^{-1}.

The two opposite jets are lunched from the inner 10^{14} cm region along the z-axis and within a half opening angle of $\alpha = 50^\circ$. By the term 'jets' we refer also to wide outflows, as we simulate here. More generally, we simulate slow-massive-wide (SMW) outflows. Although the jets that are simulated here are not observed (because the medium is optically thick), such wide outflows are commonly observed to be blown from active galactic nuclei (e.g., Arav et al. 2013). This, and the success of wide outflows to explain lobes observed in cooling flow clusters (e.g., Sternberg et al. 2007) motivate us to consider wide outflows.

The jets' launching episode lasts for 5×10^6 s = 58 day, coresponding to about one orbital period of a companion around a massive star of radius of 1 AU. The jets' initial velocity is $v_{\rm jet} = 700$ km s^{-1}, corresponding to the escape speed form a main sequence star, and the mass loss rate into the two jets together is $\dot{M}_{\rm 2jets} = 0.13M_\odot$ yr^{-1}. The high mass loss rate is assumed to occur as a companion enters or grazes the envelope of a giant star. The slow wind, dense shell, and the ejected jets start with a temperature of 1000 K. The initial jets' temperature has no influence on the results (as long as it is highly supersonic) because the jets rapidly cool due to adiabatic expansion. For numerical reasons a weak slow wind is injected in the sector $\alpha < \theta < 90^\circ$ (more numerical details are in Akashi & Soker 2013).

A new ingredient compared with our previous paper is a fast wind that starts to be blown at $t = 8\times10^6$ s. Its speed is $v_{\rm fast} = 1000$ km s^{-1} and the mass loss rate is $\dot{M}_{\rm fast} = 0.01M_\odot$ yr^{-1}. A high mass loss rate is assumed to exist as the remnant of the two merged star is out of equilibrium for some time. As we discuss below, in reality the fast wind is expected to last for a much longer time and its mass loss rate is expected to be lower. But for numerical reasons we simulate the fast wind to be a short episode just after the jets-launching phase.

3. RAPID COOLING: THE FORMATION OF RINGS

As described in section 2 there are three consecutive flow components. (1) A slowly expanding spherical shell that is assumed to be blown by the primary giant star as a result of a short and strong binary interaction. (2) Two opposite jets that are assumed to be launched by a main sequence companion that accretes at a high rate from the primary envelope. In the results to be presented here this phase lasted in the period $t = 0 - 58$ day. (3) A fast wind blown by the primary star as a result of the merger process with the secondary star, or from the contraction of the star, as in the evolution to a blue giant of the progenitor of SN 1987A. We present the interaction between these three components, but limit the presentation to emphasize the physics of the flow and the morphology.

For numerical reasons (saving resources) we launch the fast spherical wind starting at time $t = 8\times10^6$ s = 0.25 yr. However, in reality the structure formed from the interaction of the jets with the shell can evolve for tens to hundreds of year before the fast wind has its full power. For that, the present study cannot be compared quantitatively to observed objects. We limit the present study to the general morphology that can be formed by these three mass-loss episodes.

We start with the presentation of the results for the numerical simulation with $\gamma = 1.02$, that mimics radiative losses at early times (Akashi & Soker 2013). In Figure 1 we present the density maps in the meridional plane, i.e., the plane containing the jets' axis. The basic interaction of the three mass loss episodes evolves as follows. As the jets interact with the dense slow shell they inflate two opposite bubbles, with instabilities that develop in the shell (Akashi & Soker 2013). We do not present the evolution of this phase, as detailed can be seen there, but only the density at the time the fast spherical wind starts.

The fast spherical wind, which is the new addition in the present study, then interacts with the bubbles. The interaction results in a complicated flow structure and instabilities because of the shape of the bipolar structure formed by the jets. One consequence is the formation of dense rings away from the equatorial plane. The two rings can be seen as red regions (high density) away from the equatorial plane in the last panel of Figure 1: the upper ring crosses the meridional plane at that time near $(x, y) = (2.16, 5.5)$ and $(x, y) = (2.84, 5.5)$, and the lower ring crosses the meridional plane near $(x, y) = (2.16, 4.5)$ and $(x, y) = (2.84, 4.5)$, where distances are in units of 10^{15} cm. There is a large dense region in the equatorial plane as well (Akashi & Soker 2013). We do not study it. As we discuss later, it is possible that the first mass loss episode, that of the dense shell, has a mass concentration at mid-latitudes, with the result of denser outer rings and a less massive equatorial ring.

To emphasize the double-ring structure that might be revealed in observations, we present the scaled emissivity, i.e., the density square, in the meridional plane in the left panel of Figure 2. The time of the simulation is $t = 1.27$ yr, but as mentioned above this is due to numerical limitations. In reality the time after the fast wind has shaped the nebula can last for tens to hundreds of years, and even thousands of years. In the middle panel in the same figure we present the temperature, and in the right panel the velocity of the flow. From the left panel we learn that the emissivity of the thin shell around the bubble is much higher than that of the surroundings. The rings, the two outer rings and the equatorial ring, have a higher emissivity than the rest of the thin shell. Namely, in observations the rings will form a clear structure, but the thin shell will also be presence. We will come back to this later.

The contrast in density and emissivity between the rings and the rest of the shell we obtain is much lower than the contrast inferred in observations of the outer ring of SN 1987A. We find the density in the rings to be larger by a factor of about 2 relative to the rest of the shell (red versus green in the last panel of Figure 1. The density of the rings of SN 1987A is a factor of about 100 larger than the density of surroundings of the rings (Burrows et al. 1995; Panagia et al. 1996). We do not manage to account for this density ratio.

The flow becomes unstable in many place. Instabilities start from the interaction of the jets with the dense shell. In Akashi & Soker (2013) we found strong instabilities on the boundaries of the bubble, and in Akashi et al. (2015) we studies the instabilities near the equatorial plane. Here we present the instabilities after the fast wind has interacted with the dense boundary of the bubble. In Figure 3 we present the density maps in two planes parallel to the equatorial plane at three times, corresponding to the same run and last three epochs presented in Figure 1. The last panel corresponds to the plane of the upper rings. The ring might become clumpy according to our results. In reality there will be many smaller clumps, instead of several large one that are dictated by the numerical grid.

Motivated by the observations that the structure of the two outer rings of SN 1987A is displaced from the exploding star, we run simulations where the jets have been given a transverse (horizontal) velocity. Namely, a velocity component perpendicular to the jets' axis (here it is perpendicular to the z axis) has been added. Here we present results of a numerical simulation with a transverse given velocity of $v_t = 100$ km s^{-1} in the x direction. All other parameters are as in the run presented in Figures 1-3. Such a velocity can

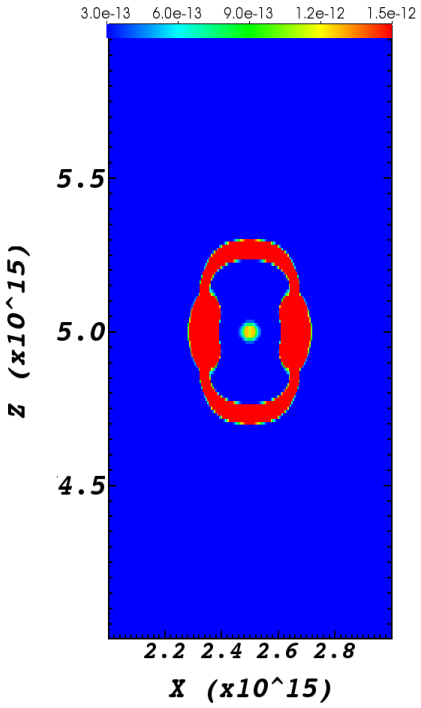

(a) $t = 0.25$ yr

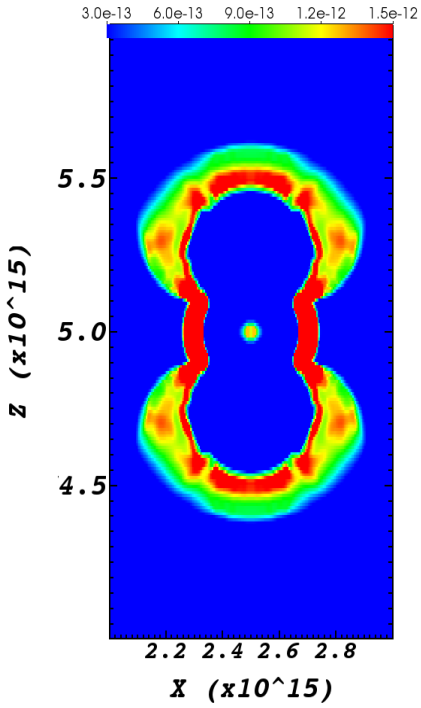

(b) $t = 0.82$ yr

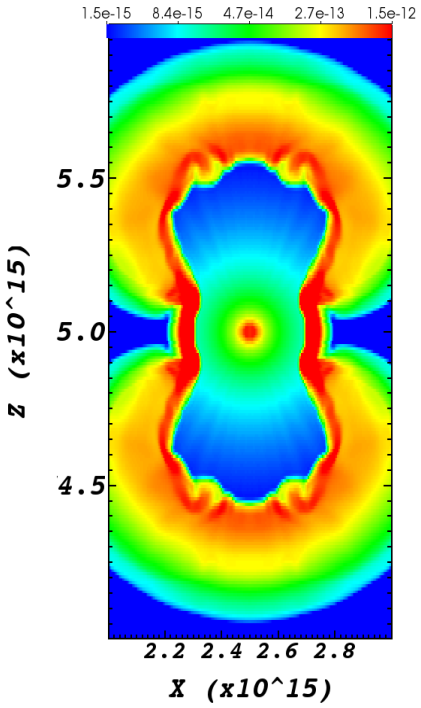

(c) $t = 1.08$ yr

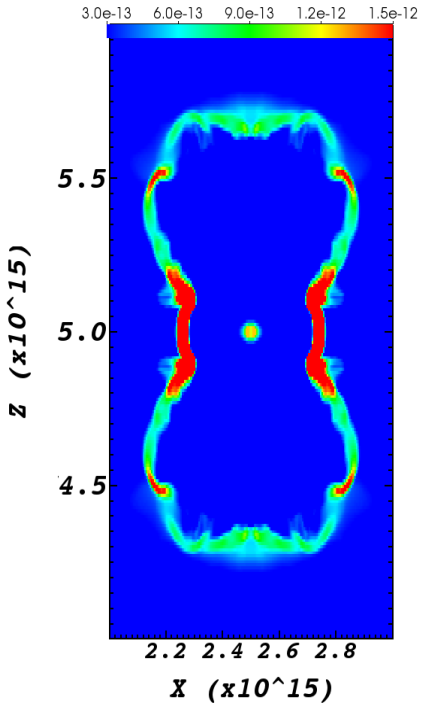

(d) $t = 1.27$ yr

Fig. 1.— The density maps in the meridional plane at four times for the $\gamma = 1.02$ run. The first panel is at the time the fast spherical winds starts. Density color coding is in units of g cm^{-3}, with a log scale in the third panel and a linear scale in the other three panels. Units on the axes are in cm. The flow that leads to the structure in the first panel is composed of two opposite jets that are injected at $r = 10^{14}$ cm along the Z axis, with a half opening angle of 50°, with an initial velocity of 700 km s^{-1}, and during the time period $t = 0$ to $t = 58$ days.

be acquired from a jets' launching episode that is shorter than the orbital period. For example, consider a companion of mass $M_2 = 2M_\odot$ orbiting a star of $20M_\odot$ at $a = 2$ AU. The orbital period is 220 day, which is about 4 times the duration of the jets' launching episode used here. The relative velocity of the two stars is about 100 km s^{-1}.

We present the results of the displaced-jets run in Figure 4. The panels present the same times and scaling as in the last three panels of Fig. 1. Rings are still obtained, with three characteristics of the displacement. (1) The line connecting the center of the two outer rings is displaced from the center. (2) The more displaced side (the right side in the panels) is fainter. This fainter side is not observed in the outer rings of SN 1987A. (3) The rings are tilted, in the sense that the more displaced side of the ring was accelerated to larger distance in the z direction. It seems the outer rings of SN 1987A do not show this tilt. Over all, with this additional transverse velocity given to the jets we do not reproduce the displacement observed in the outer rings of SN 1987A.

We also run one model where the spherical dense shell that was formed before the launching of the jets is displaced by $\Delta x_s = 1.5 \times 10^{13}$ cm in the x-direction. The jets and all other parameters as in the run presented in Figures 1-3. The results of this displaced-shell run are presented in Figure 5. Because of this displacement there is more mass per unit solid angle in the $+x$ side (right side in the figure), and hence this side is accelerated less by the jets and the fast wind. As with the case of the displaced-jets, a double-ring system with displaced and tilted rings is formed (the outer rings). A complicate structure with clumps and one place where the fast winds almost breaks out can be seen on the front of the dense shell on each side of the equatorial plane. Here again the displaced double-ring structure is tilted and the intensity along the rings varies by a large factor. These properties are not observed in the outer rings of SN 1987A.

We can summarize this section by pointing to the double-ring system we have obtained. If jets repeat themselves, several rings might be formed. The type of flow studied here might be relevant to some bipolar PNe, but we could not reproduce the properties of the outer rings of SN 1987A.

4. SLOW COOLING: FORMING MULTIPLE-LOBES

We present results of a run where we set the adiabatic index to be $\gamma = 1.1$ instead of $\gamma = 1.02$ as in the runs presented in section 3. This represents a case where the radiative losses are moderate. All other parameters are as in the run presented in Figures 1-3. In this case a larger fraction of the kinetic energy of the jets and the fast wind is transferred to thermal energy of the shocked gas, and a large hot bubble is formed, as can be seen in the density and temperature maps presented in Figures 6 and 7.

We do not obtain rings outside the equatorial plane, but rather a structure of 3 bubbles on each side of the equatorial plane is formed in the meridional plane. In 3D, the structure is of a central bubble and a torus-like bubble around it. In observations, the structure will be of three pairs of bipolar lobes. We are not aware of any PN that can be explained by this specific structure. This structure might be transients.

There are two main conclusions that we draw from this run and the one presented in section 3. (1) The nebular structure that is obtained from the three mass loss episodes is very sensitive to the radiative losses during the interaction. (2) Jets can enrich the variety of morphological structures that result from binary interaction.

5. DISCUSSION AND SUMMARY

This paper is another one in our series of papers aiming at exploring the role of jets in shaping some nebulae around evolved stars (Akashi & Soker 2008a,b; Akashi et al. 2015). The new ingredient we have added is a fast spherical wind blown after the shaping by jets. Such a wind is expected to last tens to thousands of years. Due to numerical limitations, we set the fast wind to be very short and to have a very high mass loss rate.

We mimicked radiative cooling by using a low ($\gamma = 1.02$; Figs. 1-5) and moderate ($\gamma = 1.1$; Figs. 6-7) adiabatic indices. When cooling is rapid enough, we obtained a structure of three rings, that are seen as in red color in the bottom-right panel of Fig.1: a massive ring in the equatorial plane, and two outer rings, one at each side of the equatorial plane. Each outer ring ia part of a dense shell on the boundary of the bubble. The rings are much denser than regions outside and inside this shell, but not much denser than gas in the shell. As such, our model with the parameters used cannot reproduce the outer rings of SN 1987A that are much denser than their surroundings.

The line connecting the two outer rings of SN 1987A is displaced with respect to the star that exploded. We have tried to reproduce the displacement of the rings by displacing the spherical shell and by adding transverse velocity to the jets. These did not reproduce all properties of the outer rings.

Morris & Podsiadlowski (2009) could produce many of the properties of the outer rings without jets. They rather assumed that more mass was lost at a mid latitude at each side of the equatorial plane. This is based on their study of the merger process of two stars Morris & Podsiadlowski (2006). It is possible that the formation of outer rings with a large density contrast requires that there will be a high mass loss rate at mit-latitude, as assumed by Morris & Podsiadlowski (2007) and Morris & Podsiadlowski (2009) for the progenitor of SN 1987A, and as Smith (2006) found for the Great Eruption of η Carinae that formed its bipolar nebula, the Homunculus. Our model includes three mass loss episodes: a spherical shell, jets, and a spherical fast wind. The next step should be to replace the spherical shell by a shell with enhanced mass loss at mid-latitudes.

We could produce outer rings that might be applicable in some PNe when radiative cooling in our model was significant, as we modeled by taking $\gamma = 1.02$. When the radiative losses are moderate, as we simulated by taking $\gamma = 1.1$, outer rings are not formed. Instead a complicated structure of lobes arises. Further comparison with observed specific PNe requires to tune the parameters, which is beyond our scope.

Our main result is in further emphasizing the large variety of bipolar morphological structures around evolved stars that can be shaped by jets, and in particular to attributing a role to the fast wind.

ACKNOWLEDGEMENT
This research was supported by the Asher Fund for Space Research at the Technion.

REFERENCES

Akashi, M., Sabach, E., Yogev, O., & Soker, N. 2015, MNRAS, 453, 2115

Akashi, M., & Soker, N. 2008a, MNRAS, 391, 1063

Akashi, M., & Soker, N. 2008b, New A, 13, 157

Akashi, M., & Soker, N. 2013, MNRAS, 436, 1961

Arav, N., Borguet, B., Chamberlain, C., Edmonds, D., & Danforth, C. 2013, MNRAS, 436, 3286

Balick, B., Huarte-Espinosa, M., Frank, A., Gomez, T., Alcolea, J., Corradi, R. L. M., & Vinkovic, D. 2013, ApJ, 772, 20

Boffin, H. M. J., Miszalski, B., Rauch, T., Jones, D., Corradi, R. L. M.; Napiwotzki, R., Day-Jones, A. C., & Koppen, J. 2012, Science, 338, 773

Burrows, C. J., Krist, J., Hester, J. J., et al. 1995, ApJ, 452, 680

Chen, Z., Nordhaus, J., Frank, A., & Blackman, E. G. 2016, arXiv:1602.06142

Cohen, M., Van Winckel, H., Bond, H. E., & Gull, T. R. 2004, AJ, 127, 2362

Corradi, R. L. M., & Schwarz, H. E. 1993, A&A, 268, 714

Crotts, A. P. S., & Heathcote, S. R. 2000, ApJ, 528, 426

De Marco, O. 2015, in "Physics of Evolved Stars 2015 - A conference dedicated to the memory of Olivier Chesneau", in press

Dennis, T. J., Cunningham, A. J., Frank, A., Balick, B., Blackman, E. G., Mitran, S. 2008, ApJ, 679, 1327

Dennis, T. J., Frank, A., Blackman, E. G., De Marco, O., Balick, B., & Mitran, S. 2009, ApJ, 707, 1485

Fryxell, B., Olson, K., Ricker, P., et al. 2000, ApJS, 131, 273

García-Díaz, M. T., López, J. A., García-Segura, G., Richer, M. G., & Steffen, W. 2008, ApJ, 676, 402

García-Segura, G., López, J. A., & Franco, J. 2005, ApJ, 618, 919

Huarte-Espinosa, M., Frank, A., Balick, B., Blackman, E. G., De Marco, O., Kastner, J. H., & Sahai, R. 2012, MNRAS, 424, 2055

Kwok, S., & Su, K. Y. L. 2005, ApJ, 635, L49

Lee, C.-F., Hsu, M.-C., & Sahai, R. 2009, ApJ, 696, 1630

Maran, S. P., Sonneborn, G., Pun, C. S. J., Lundqvist, P., Iping, R. C., & Gull, T. R. 2000, ApJ, 545, 390

Martínez González, M. J., Asensio Ramos, A., Manso Sainz, R., Corradi, R. L. M., & Leone, F. 2015, A&A, 574, A16

Morris, M. 1987, PASP, 99, 1115

Morris, T., & Podsiadlowski, P. 2006, MNRAS, 365, 2

Morris, T., & Podsiadlowski, P. 2009, MNRAS, 399, 515

Morris, T., & Podsiadlowski, P. 2007, Science, 315, 1103

Panagia, N., Scuderi, S., Gilmozzi, R., Challis, P. M., Garnavich, P. M., & Kirshner, R. P. 1996, ApJ, 459, L17

Riera, A., Velázquez, P. F., Raga, A. C., Estalella, R., & Castrillón, A. 2014, A&A, 561, A145

Sahai, R., Dayal, A., Watson, A. M., et al. 1999, AJ, 118, 468

Sahai, R., Nyman, L.-Å., & Wootten, A. 2000, ApJ, 543, 880

Sahai, R., & Trauger, J. T. 1998, AJ, 116, 1357

Smith, N. 2006, ApJ, 644, 1151

Soker, N. 1998, ApJ, 496, 833

Soker, N. 2002a, ApJ, 577, 839

Soker, N. 1999, MNRAS, 303, 611

Soker, N. 2002b, MNRAS, 330, 481

Soker, N. 2005, AJ, 129, 947

Soker, N. 2007, ApJ, 661, 490

Soker, N. 2016, MNRAS, 455 1584

Soker, N., & Kashi, A. 2012, ApJ, 746, 100

Soker, N., & Rappaport, S. 2000, ApJ, 538, 241

Sternberg, A., Pizzolato, F. & Soker N. 2007, ApJ, 656, L5

Sugerman, B. E. K., Crotts, A. P. S., Kunkel, W. E., Heathcote, S. R., & Lawrence, S. S. 2005, ApJ, 627, 888

Tanaka, T., & Washimi, H. 2002, Science, 296, 321

Thomas, J. D., Witt, A. N., Aufdenberg, J. P., Bjorkman, J. E., Dahlstrom, J. A., Hobbs, L. M., & York, D. G. 2013, MNRAS, 430, 1230

Tocknell, J., De Marco, O., & Wardle, M. 2014, MNRAS, 439, 2014

Van Winckel, H. 2004, Mem. Soc. Astron. Italiana, 75, 766

Velázquez, P. F., Steffen, W., Raga, A. C., Haro-Corzo, Sinhu; Esquivel, Alejandro; Cant, Jorge; Riera, Angels 2011, ApJ, 734, 57

Velázquez, P. F., Riera, A., Raga, A. C., & Toledo-Roy, J. C. 2014, ApJ, 794, 128

Zijlstra, A. A. 2015, Rev. Mexicana Astron. Astrofis., 51, 221

This preprint was prepared with the AAS LaTeX macros v5.2.

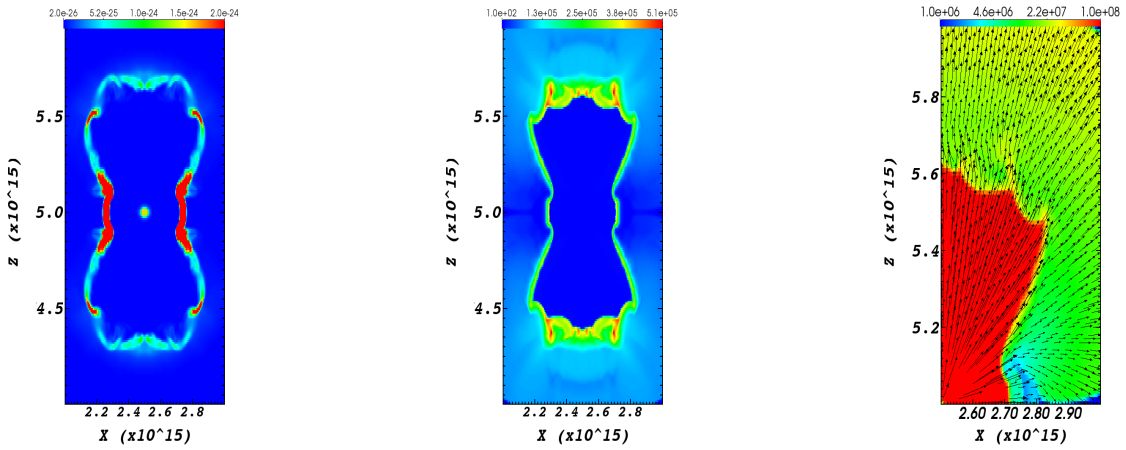

(a) $t = 1.27$ yr (b) $t = 1.27$ yr(log scale) (c) $t = 1.27$ yr

Fig. 2.— Some quantities in the meridional plane at time $t = 1.27$ yr for the run presented in Figure 1. Left: The squared of the density in g^2 cm^{-6}. Middle: The temperature map in K. Right: The velocity magnitude map (log scale in cm s^{-1}) with the velocity direction depicted by the arrows. The length of the arrows represents four velocity regimes, $0-100$ km s^{-1}, $100-200$ km s^{-1}, $200-600$ km s^{-1}, and $600-1000$ km s^{-1}. To better resolve the arrows we show only one quarter of the meridional plane.

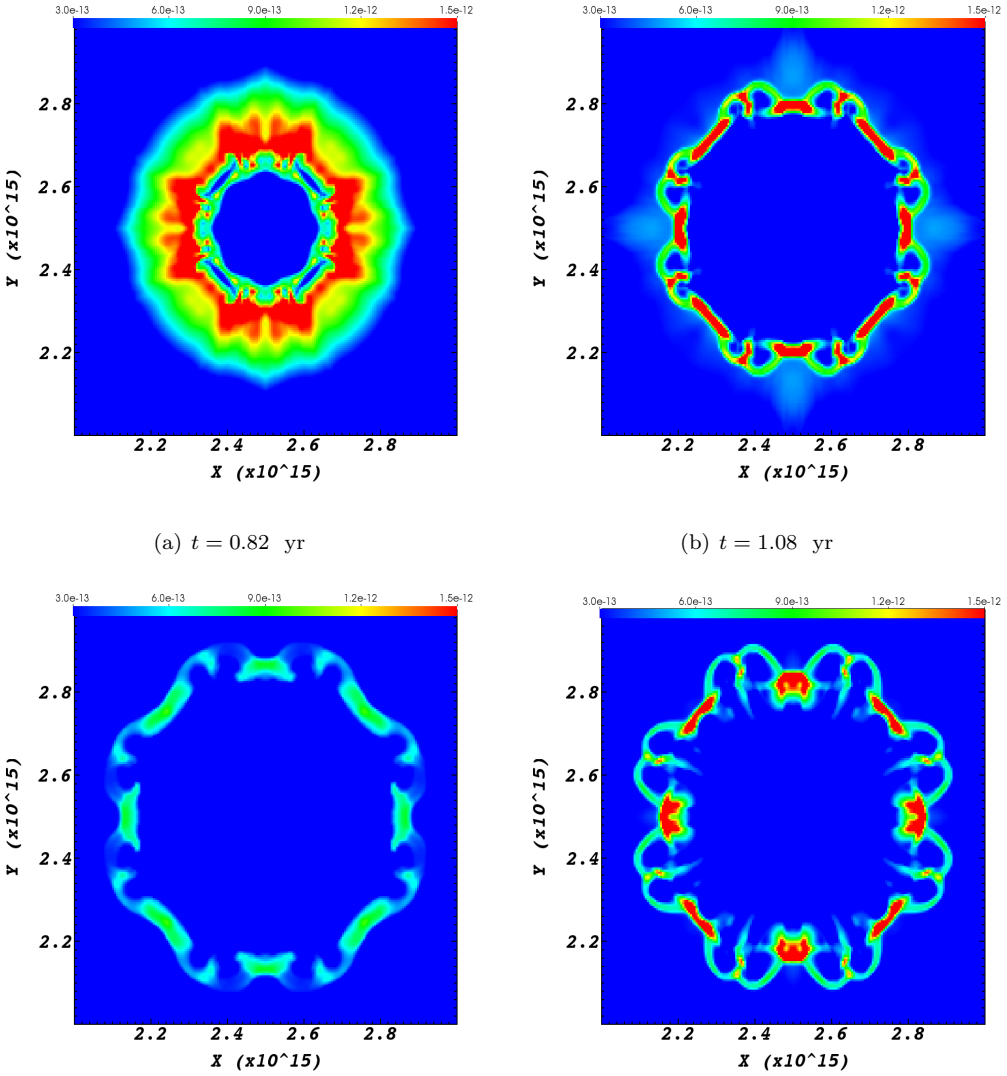

(a) $t = 0.82$ yr

(b) $t = 1.08$ yr

(c) $t = 1.27$ yr

(d) $t = 1.27$ yr

Fig. 3.— The density maps at 3 times of the $\gamma = 1.02$ run presented in Figures 1 and 2, but in planes parallel to the equatorial plane. The first three panels present maps at three times in the $z = 5.4 \times 10^{15}$ cm plane (a distance of 0.4×10^{15} cm from the equatorial plane). The fourth panel is at the time $t = 1.27$ yr but in the $z = 5.5 \times 10^{15}$ cm plane. Color coding is in g cm^{-3} and units on the axes are in cm. The panels emphasize the development of instabilities in the shell around the low-density bubble. The fine detail structures of the instabilities are determined also by the numerical grid, but their existence is physical.

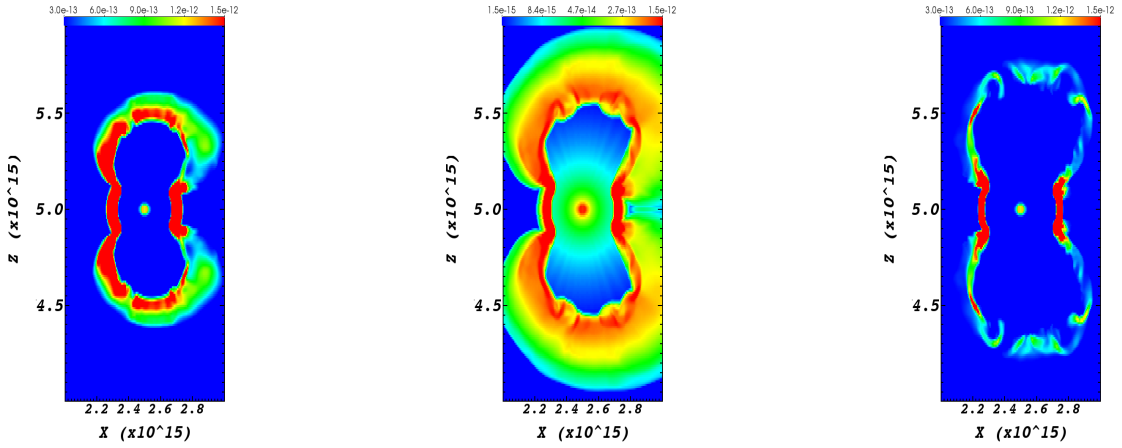

(a) $t = 0.82$ yr (b) $t = 1.08$ yr (c) $t = 1.27$ yr

Fig. 4.— Same as last three panels of Fig. 1, but the jets have been injected with an initial extra velocity of $v_t = 100$ km s^{-1} in the x direction. Otherwise all parameters are as in the run presented there.

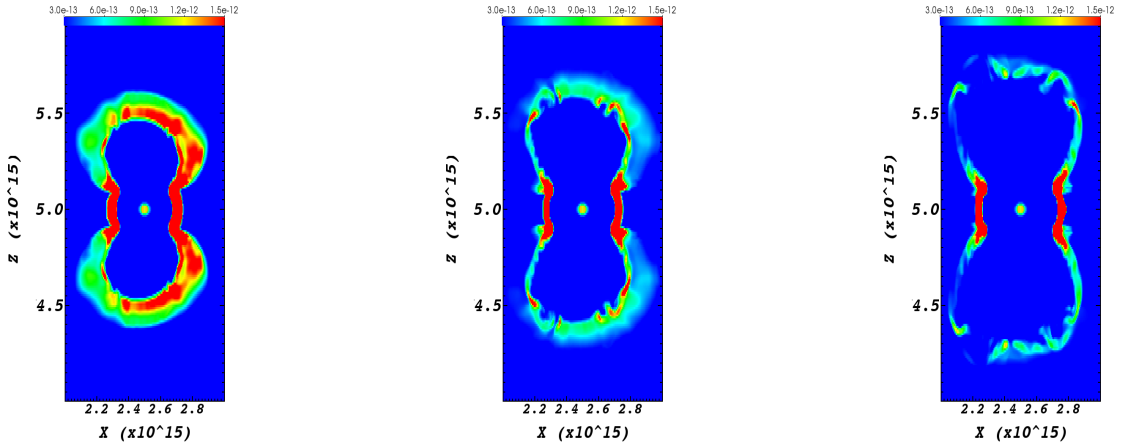

(a) $t = 0.82$ yr (b) $t = 1.08$ yr (c) $t = 1.27$ yr

Fig. 5.— Same as last three panels of Fig. 1, but the spherical shell that is placed before the jets are launched is displaced in the x-direction by $\Delta x_s = 1.5 \times 10^{13}$ cm. Otherwise all parameters are as in the run presented there.

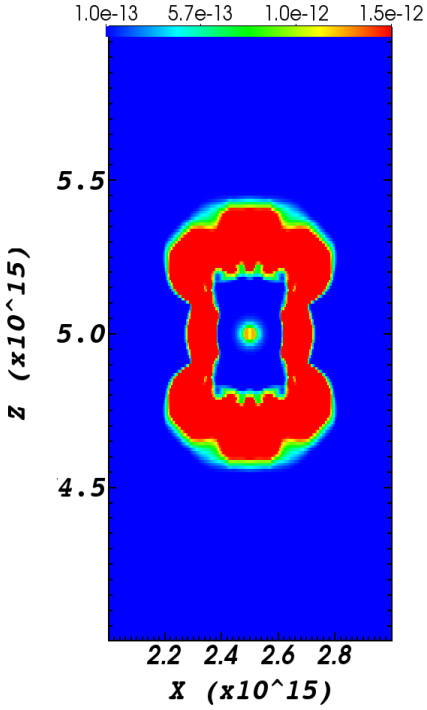

(a) $t = 0.45$ yr

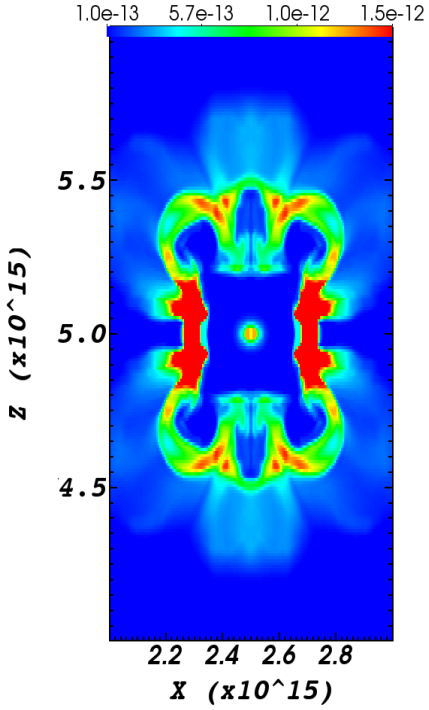

(b) $t = 0.82$ yr

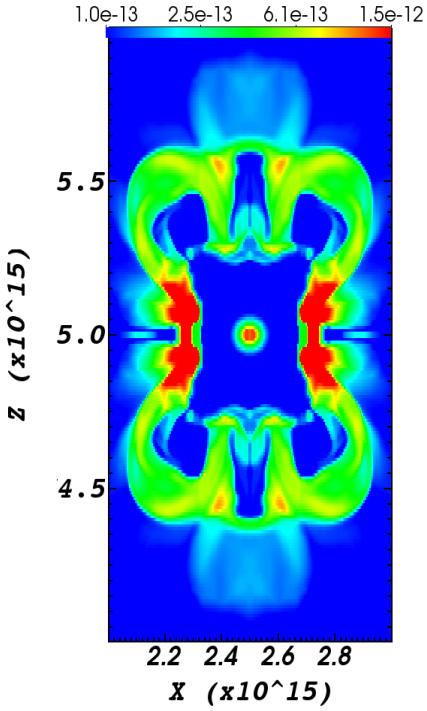

(c) $t = 1.08$ yr

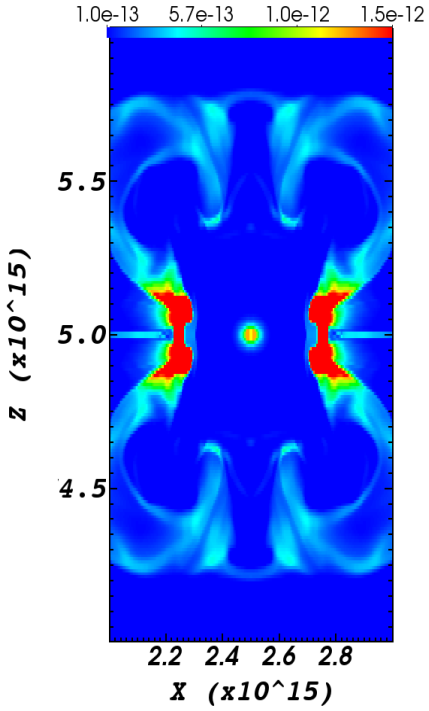

(d) $t = 1.27$ yr

Fig. 6.— The density maps in the meridional plane as in Figure 1, but taking the adiabatic index to be $\gamma = 1.1$, and at different times as indicatred. Other parameters of the simulation are as in the run presented in Figures 1-3. Density color coding is in units of g cm^{-3} and in a linear scale. Units on the axes are in cm.

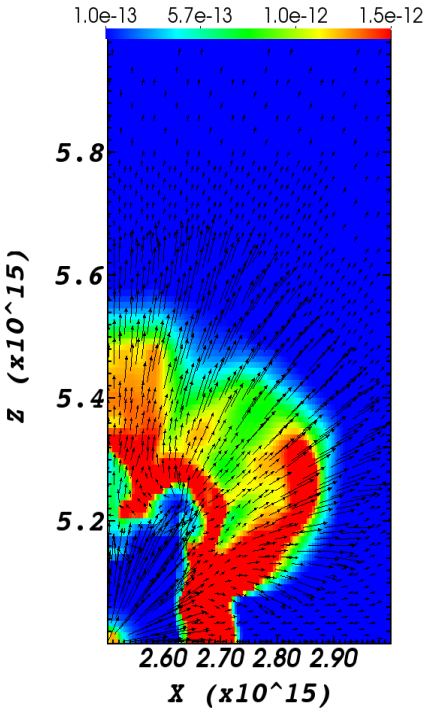

(a) $t = 0.61$ yr

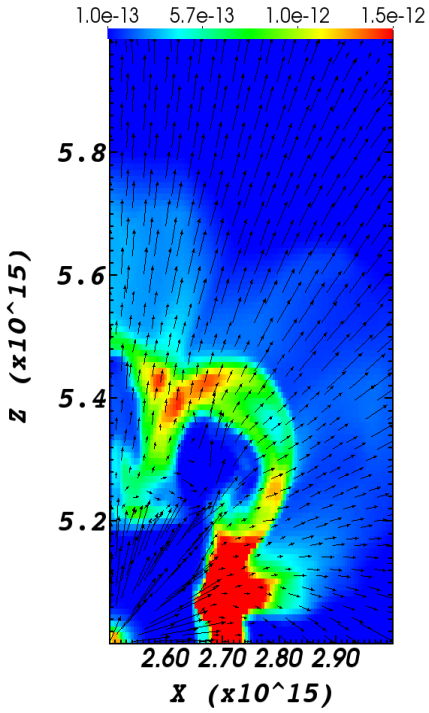

(b) $t = 0.82$ yr

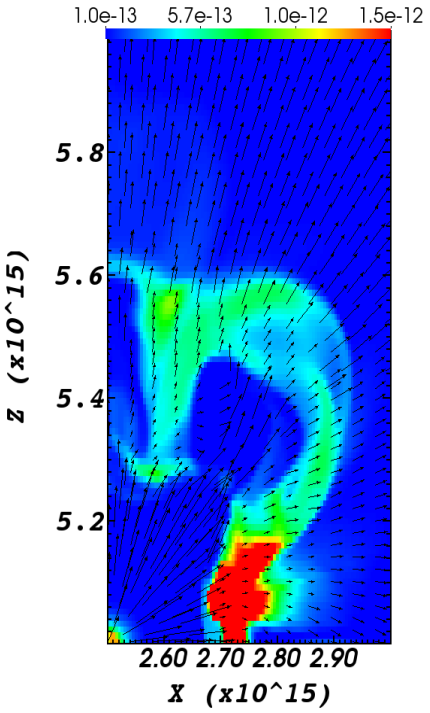

(c) $t = 1.08$ yr

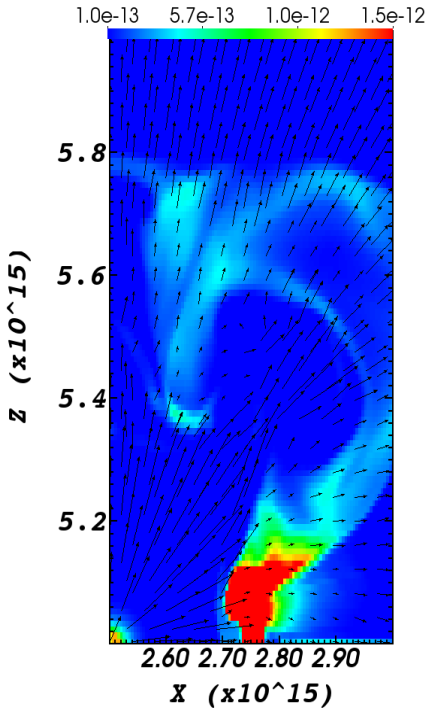

(d) $t = 1.27$ yr

Fig. 7.— The density maps and velocity arrows at four times corresponding to the four panels presented in Figure 6. The length of the arrows represents four velocity regimes, $0 - 100$ km s^{-1}, $100 - 200$ km s^{-1}, $200 - 600$ km s^{-1}, and $600 - 1000$ km s^{-1}. Only one quarter of the meridional plane is shown.